

IMECE2003-41577

EFFECTS OF ABSOLUTE PRESSURE ON FLUID SLIP IN A HYDROPHOBIC MICROCHANNEL

Derek C. Tretheway and Carl D. Meinhart
Department of Mechanical and Environmental Engineering
University of California Santa Barbara
Santa Barbara, CA 93106
Email: meinhart@engineering.ucsb.edu

ABSTRACT

This work examines the effects of absolute pressure on fluid slip in a hydrophobic microchannel. Previous experiments with hydrophobic surfaces have indicated the presence of an apparent fluid slip. The mechanism responsible for the apparent fluid slip observed by Pit. et. al. (Phys. Rev. Lett., **85**, 980-983), Zhu and Granick (Phys. Rev. Lett., **87**, 096105), and Tretheway and Meinhart (Phys. of Fluids, **14**, L9-L12) is unknown. Recently, Tyrell and Attard () have observed the presence of nanobubbles on a hydrophobic surface. Modeling these nanobubbles as a thin gas layer and solving for the velocity profile between two infinite parallel plates yields an apparent fluid slip consistent with the experimentally observed results. As the slip length is highly dependent on the nanobubble or gas layer thickness, increases in absolute pressure should decrease the bubble size and reduce the measured slip. This work explores the proposed mechanism by measuring velocity profiles and calculating slip lengths at varying absolute pressures.

NOMENCLATURE

h	half height of plate separation
dp/dx	pressure drop
v	velocity
x	streamwise direction
y	spanwise direction
β	slip length
δ	air gap thickness
μ_a	air viscosity
μ_w	water viscosity

INTRODUCTION

The current development of microfluidic devices for micro-total analysis systems has led to research focused on fluid flow at the microscale. Since the surface to volume ration depends inversely on the lengthscale, the importance of boundary conditions increases as the lengthscale decreases. Recently, several researchers have suggested that the generally accepted no-slip boundary condition may not be suitable at both the micro- and nano-scale. Ruckenstein and Rajora [1] investigated fluid slip in glass capillaries with surfaces made repellent to the flowing liquid. Their experimental results of pressure drop indicate larger slip than that predicted by chemical potential theory, where slip is proportional to the gradient in the chemical potential. The results suggest that slip occurs over a gap near the surface rather than directly on the solid surface, and the gap forms when a hydrophobic liquid flows over a hydrophilic surface and vice versa. They suggest the gap may be increased in thickness by the release of gases entrained in the flowing liquid and/or the desorption of soluble gases. Their results, however, are inferred from pressure drop-flow measurements and not direct measurement of the fluid velocities. Computationally, Barrat and Bocquet [2] expect significant slip in nanoporous medium when the liquid is sufficiently non-wetting, which increases the effective permeability of the nanoporous medium. Their predictions are experimentally justified by Churaev et. al. [3] who postulated slip at the wall to recover the viscosity of water for water flow in thin ($<1\mu\text{m}$) hydrophobic capillaries. Pit et. al. [4] observe fluid slip for hexadecane between two rotating parallel disks with a gap of 190 microns. By following the movement of a photo-bleached test section, they measure no slip when the surfaces are coated with perfluorodecanetrichlorosilane, a slip length of approximately 170nm for bare sapphire, and a slip length of 400nm for an octadecyltrichlorosilane (OTS) coating.

They conclude that slip depends on both the interfacial energy and surface roughness. At a much smaller length scale, Craig et. al. [5] calculate the drainage force for a sphere approaching a solid, flat wall. They measure slip lengths up to 20nm for aqueous sucrose solutions that have advancing and receding contact angles of 70 and 40 degrees respectively. They conclude that the slip length depends non-linearly on the approach rate of the sphere. Zhu and Granick [6] experimentally observe fluid slip in an oscillating surface force apparatus. For cylinder separations from approximately 10-200nm, they measure slip lengths of up to 2.5 μm for water between octadecyltriethoxysilane (OTE) surfaces, 1.5 μm for tetradecane between OTE surfaces, and 0.9 μm for tetradecane between mica surfaces. Their results suggest a strong dependence between the velocity gradient and magnitude of the slip, a critical shear rate for onset of fluid slip, and an increase in the slip length as the separation between the cylinders decreases. Their conclusions, however, are inferred from discrepancies between the measured normal force and expected normal force assuming no-slip, and are not measured directly. More recently, Zhu and Granick [7] examine the relative importance of surface roughness and fluid-surface interactions in determining the appropriate boundary condition. For similar, poorly wetting surfaces the critical shear rate to observe deviations from force predictions assuming no-slip increased nearly exponentially with increasing surface roughness. They conclude that local intermolecular interactions are dominate when surfaces are very smooth, but are otherwise negligible at sufficient surface roughness. Tretheway and Meinhart [8] measured fluid velocities in hydrophilic and hydrophobic microchannels by micron resolution particle image velocimetry ($\mu\text{-PIV}$). Their results showed a significant fluid velocity near a hydrophobic microchannel wall and no-slip for a hydrophilic surface. A slip length of 0.92 microns was estimated.

The mechanism for the generation of the apparent fluid slip observed by Tretheway and Meinhart [8] is unknown. Ruckenstein and Rajora [1] suggest that fluid slip may develop from entrained and soluble gases forming a gap near the wall. Recently, Tyrell and Attard [9] imaged, with an atomic force microscope, a hydrophobic glass surface submerged in water. Their results showed the presence of pancake shaped, 20 to 30 nm thick nano-bubbles completely covering the surface. In addition, they showed that the hydrophobic surface acts as a nucleation site pulling dissolved gasses out of solution. Within 10 to 20 minutes after scraping the surface clean, the surface was once again completely covered with nano-bubbles.

In Tretheway and Meinhart [8], velocity measurements were made for deionized water flowing over a hydrophobic surface. No treatment of the water was conducted to remove dissolved or entrained gasses. To determine if dissolved gasses could generate the apparent fluid slip, we examine analytically flow between to infinite parallel plates assuming nano-bubbles form an effective air gap near the wall. From this simple one-dimensional model we can calculate the bubble height or air gap required to generate measured slip lengths assuming Navier's hypothesis effectively describes a thin air gap at the surface. Navier's hypothesis states that the velocity at a surface is proportional to the shear rate at the surface with the proportionality constant equal to the slip length β . For two phase flow between two infinite parallel plates with a thin air gap of thickness, δ , at the wall and a fluid layer of thickness $2h$,

the solution for the velocity in the water phase assuming Stokes flow for both phases, no stress at the centerline, continuity of stress and velocity at the air-water interface, and no-slip at the air-wall interface is

$$v = \frac{1}{2\mu_w} \left(\frac{dp}{dx} \right) \left[y^2 - 2hy - 2 \frac{\mu_w}{\mu_a} h\delta - \frac{\mu_w}{\mu_a} \delta^2 \right] \quad (1)$$

where μ_a and μ_w are the viscosity of air and water respectively, $(-dp/dx)$ is the pressure drop, $y=0$ at the air water interface, and $y=-\delta$ at the wall. Assuming Navier's hypothesis effectively describes the thin air gap at the wall, we set the velocity at the wall equal to the slip length times the shear rate at the wall and obtain an equation for the slip length as a function of the air gap thickness and the plate separation

$$\beta = \frac{\mu_w}{\mu_a} \left(\frac{\delta^2}{2h} + \delta \right) \quad (2)$$

Figure 1 shows the air gap thickness required for a given plate separation to generate a given slip length. As the plate separation decreases the slip length generated by a given air gap thickness increases. At very small separations the slip length is strongly dependent on the air gap thickness. In this work we calculate a slip length of 0.92 μm . With 30 μm channels, this yields a required air gap thickness of approximately 18nm. This thickness is consistent with the measured bubble heights of Tyrell and Attard [9]. In addition, when surfaces are hydrophobic, Zhu and Granick [6] calculated slip lengths of approximately 2.5 μm for a 20nm separation. The corresponding bubble height of $\sim 20\text{nm}$ is consistent with the required bubble height in this work and the measured values of Tyrell and Attard¹¹. However, as shown in Fig. 1, Zhu and

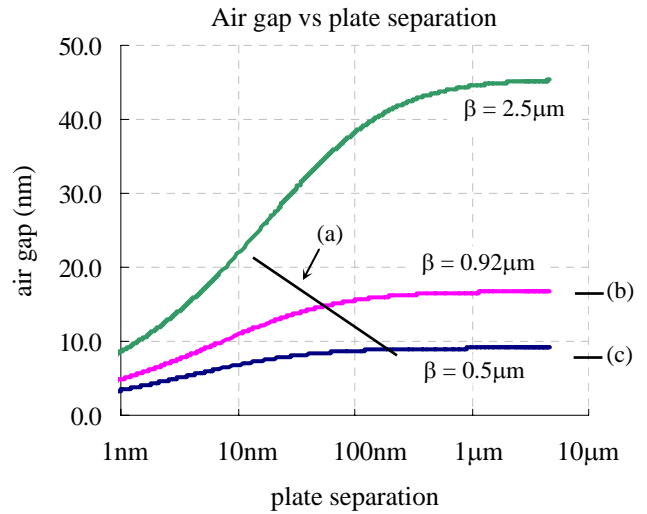


Figure 1. Air gap thickness as a function of plate separation to produce a given slip length. Locations of experimentally measured slip lengths indicated. (a) Zhu and Granick (2001), (b) Tretheway and Meinhart (2002), and (c) Pit et. al. (2000). Tyrell and Attard (2001) measured nano-bubble heights of 20-30nm.

Granick [6] reported a range of slip lengths with smaller slip lengths at larger separations. This yields a range of bubble

heights from approximately 8 to 20nm. Pit et. al. [4] calculate a slip length of approximately 400nm for a 190 μm separation, which would require a bubble height of 9nm. These results suggest that the measured apparent fluid slip may develop from an effective air gap as a result of dissolved or entrained gasses accumulating on hydrophobic surfaces.

In this work, we examine the effects of absolute pressure on the apparent fluid slip of water flowing through a hydrophobic microchannel and examine the proposed mechanism of nano-bubbles (or gas layer) generating the apparent fluid slip.

EXPERIMENTS

In this section, we review the experimental system and techniques for measuring fluid flow through hydrophilic and hydrophobic microchannels. Details of the techniques and experimental apparatus can be found in Tretheway and Meinhart [8].

Velocities were measured by micron-resolution particle image velocimetry ($\mu\text{-PIV}$) in 30 μm deep by 300 μm wide extruded glass microchannels trimmed to a length of 8.25cm. Measurements were made 4 to 4.5cm from the edge to eliminate possible entrance effects and to ensure a fully developed flow profile. Deionized water seeded with 300nm fluorescent particles was injected into the channel by a gravity feed system at a flow rate of approximately 200 $\mu\text{l/hr}$. Two channel types were examined, hydrophilic and hydrophobic. An untreated glass channel is naturally hydrophilic. Hydrophobic microchannels are created by coating the walls with octadecyltrichlorosilane (OTS). The smooth and robust monolayer is approximately 2.3nm thick with a roughness of 2-3 angstroms. The OTS layer thickness is less than 1/10000th the depth of the microchannel. Two images separated by 150 μs were captured on a cooled, interline CCD camera and analyzed with PIV software developed by Steve Wereley (currently at the Dept. of Mechanical Eng., Purdue University). The interrogation region is 128 x 8 pixels (streamwise to spanwise), which yields a spatial resolution of 14.7x0.9x1.8 μm with velocity measurements obtained to within 450nm of the wall. The out of plane measurement depth is approximately 1.8 μm . To increase signal-to-noise, 49 image pairs are cross correlated. The resulting correlation functions are then averaged before peak detection, following the algorithm given by Meinhart et. al. [10].

Velocity measurements are taken in the mid-plane of the channel (15 μm from the bottom) near the side wall. The field of view is aligned such that a section of the wall is included in each image. Since there are no particles in the wall, the resulting correlations for that region produce erroneous velocity vectors with magnitudes and directions that are inconsistent with the known direction of flow. The wall location is then set at the point at which the velocity vectors are erroneous. The uncertainty of the wall location is approximately 450nm.

To vary the absolute pressure while maintaining a constant flow rate, the feed and waste reservoirs are simultaneously connected to a pressurized nitrogen tank. The absolute pressure is then controlled by the regulator attached to the nitrogen tank. A pressure gauge is installed at the reservoirs to monitor the absolute pressure. A Validyne pressure transducer is connect across the flow channel to measure the pressure drop.

Velocity profiles

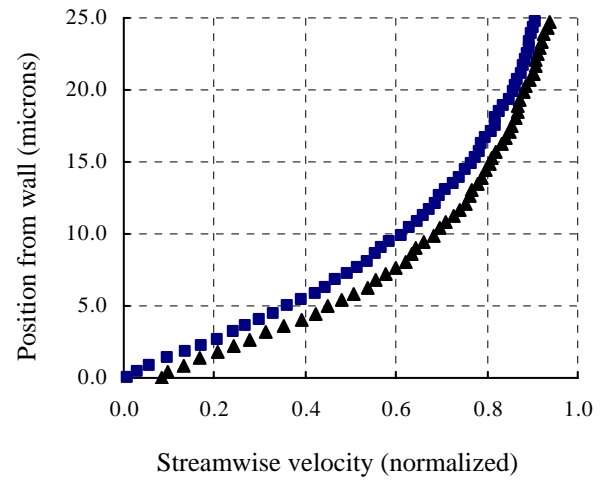


Figure 2. Experimental velocity profiles for flow over a hydrophilic (blue squares) and hydrophobic (black triangles) microchannel surface. The velocity profiles are normalized with the free-stream velocity.

RESULTS/DISCUSSION

Figure 2 shows the average velocity profile for flow near the wall for hydrophilic (squares) and hydrophobic (triangles) microchannel surfaces as reported in Tretheway and Meinhart [8]. The velocity profiles are normalized by the free-stream velocity. For a hydrophilic surface (squares), Fig. 2 shows the velocity approaching its free-stream value at 25 μm from the wall and smoothly decreasing to zero at the wall. This profile is consistent with the analytical solution for flow through a rectangular duct with a finite aspect ratio, assuming the no-slip boundary condition. For flow through a hydrophobic microchannel, the velocity profile is significantly different. While Figure 2 shows the hydrophobic velocity profile (triangles) near its free-stream value at 25 μm and decreasing towards the wall, a finite and significant velocity is measured within 450nm above the wall. This slip velocity is approximately 8.5% of the free-stream velocity, and effectively shifts the entire velocity profile when compared with the no-slip profile (squares). As a result, the velocity 25 μm from the wall in a hydrophobic microchannel is approximately 95% of the free-stream velocity, compared with 90% for a microchannel that is hydrophilic. Thus, a monolayer of hydrophobic molecules with a thickness of less than 23 angstroms significantly affects the velocity profile even out to a distance of 25 microns from the wall.

The results of Fig. 2 provide a direct measurement of fluid slip for water flowing over a hydrophobic surface, and confirm the no-slip boundary condition for water flowing over a hydrophilic surface. From these measurements we calculate a slip length, β , of approximately 0.92 μm . This is consistent with the work by Zhu and Granick [7] and Pit et. al. [5] who report slip lengths up to 2 μm .

Figure 3 shows the preliminary measured profiles for flow through a hydrophilic channel at various absolute pressures above atmospheric. The measurement plane and location are identical for each velocity profile. As expected, the velocity profiles show no-slip at the microchannel walls. Interestingly, the velocity profiles do vary with absolute pressure. As the

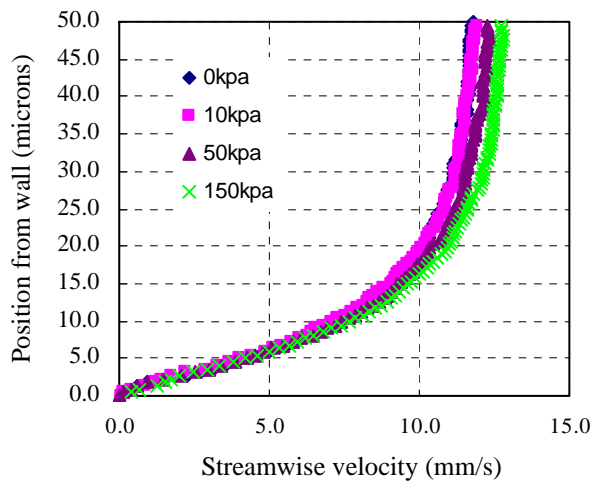


Figure 3. Velocity profiles for flow through a hydrophilic microchannel. Legend indicates the absolute pressure above atmospheric.

absolute pressure increases the free stream velocity and thus flow rate increases. This increase occurs even though the measured pressure drop remains constant or slightly decreases. Possible reasons for the increase flow rate may include trapped bubbles influencing the flow into and out of the microchannel or expansion of the channel due to the increased pressure. The cause of the increased flow rate is currently being explored.

Flows through hydrophobic microchannels are currently being conducted. In addition, the range of absolute pressure to be examined is being expanded.

CONCLUSIONS

In this work we examine the effects absolute pressure has on the velocity profiles through hydrophilic and hydrophobic microchannels while maintaining a constant pressure drop across the microchannels. As expected, preliminary results of hydrophilic channels show no change in the no-slip boundary condition. Experiments with hydrophobic surfaces are currently being conducted.

ACKNOWLEDGMENTS

This work is supported by Grant Nos. NSF CTS-9874839, NSF ACI-0086061, and DARPA/Air Force 30602-00-2-0609.

REFERENCES

- ¹Ruckenstein, E. and Rajora, P. (1983) "On the No-Slip Boundary Condition of Hydrodynamics". *J. of Colloid and Interface Science*, **96**, 488-491.
- ²Barrat, J. and Bocquet, L. (1999) "Large Slip Effect at a Nonwetting Fluid-Solid Interface". *Physical Review Letters*, **82**, 4671-4674.
- ³Churaev, N., Sobolev, V., and Somov, A. (1984) "Slippage of Liquids Over Lyophobic Solid Surfaces". *J. of Colloid and Interface Science*, **97**, 574-581.
- ⁴Pit, R., Hervet, H., and Leger, L. (2000) "Direct Experimental Evidence of Slip in Hexadecane: Solid Interfaces". *Phys. Rev. Lett.*, **85**, 980-983.
- ⁵Craig, V., Neto, C., and Williams, D. (2001) "Shear-Dependent Boundary Slip in an Aqueous Newtonian Liquid". *Phys. Rev. Lett.* **87**, 054504.
- ⁶Zhu Y., and Granick S. (2001) "Rate-Dependent Slip of Newtonian Liquids at Smooth Surfaces". *Phys. Rev. Lett.* **87**, 096105.
- ⁷Zhu, Y., and Granick, S. (2002) "Limits of Hydrodynamic No-Slip Boundary Condition". *Phys. Rev. Lett.* **88**, 106102.
- ⁸Tretheway, D. and Meinhart, C. (2002) "Apparent Fluid Slip at Hydrophobic Microchannel Walls". *Physics of Fluids* **14**, L9-L12.
- ⁹Tyrell, J. and Attard, P. (2001) "Images of Nanobubbles on Hydrophobic Surfaces and Their Interactions". *Physical Review Letters* **87**, 176104.
- ¹⁰Meinhart, C., Wereley, S., and Santiago, J. (2000) "A PIV Algorithm for Estimating Time-Averaged Velocity Fields". *J. Fluids Eng.* **122**, 285.